High Ionic Charges in Field-Evaporating 5*d* Transition Metals*

Erwin W. Müller and S. V. Krishnaswamy
Department of Physics, The Pennsylvania State University, University Park, Pennsylvania 16802
(Received 9 August 1976)

An energy-focused time-of-flight atom probe has been used in a search for highly charged ions of field-evaporating 5*d* transition metals. Maximum abundances of mostly new ion species were 1×10^{-5} for W^{6+}, 2.3×10^{-4} for W^{5+}, 2×10^{-4} for Ta^{5+}, 6.7×10^{-3} for Hf^{4+}, 2×10^{-2} for Re^{4+}, 5×10^{-5} for Ir^{4+}, 5×10^{-2} for Pt^{3+}, and 6×10^{2} for Au^{3+}. Thus for the group Hf, Ta, and W, all 6*s* and 5*d* electrons may be coming off, while for Re to Au, at most only the 6*s* electron(s) and one pair of 5*d* electrons are removed.

Thirty-five years after the discovery[1] of field desorption, the originally suggested image-potential model[1,2] which assumes that the already ionized surface atom has to overcome the Schottky hump still seems to give a good representation of the data.[3,4] The intersection model proposed by Gomer[5] suggests that ionization occurs beyond the position of the Schottky hump. McKinstry[6] has discussed which model should be preferred under certain conditions. In spite of their limitation to one-dimensional potentionals, both give for many metals the correct experimentally established evaporation fields, on the assumption that singly or doubly charged ions come off the surface.

However, higher charges were seen for the refractory metals with the advent of the time-of-flight (TOF) atom probe,[7] in which nanosecond pulses are used for field evaporation. Tungsten, rhenium, and tantalum produced threefold and fourfold charged ions, and iridium twofold and threefold ones,[8-10] with the abundance of the higher-charged ion always less but increasing with the evaporation field or evaporation rate.

While random artifact signals and an inadequate mass resolution of the conventional straight TOF atom probe limit the detection of ion species to an abundance of the order of 0.1 to 1%, our energy-deficit–compensated atom probe[11] allowed us to search for rare higher-charged ions. From earlier observations with the atom probe and the low-resolution gated field-desorption microscope,[12,13] it was known that W^{4+} and Ir^{3+} ions are preferentially obtained from certain narrow crystallographic regions, along the [111] and [100] zones of bcc W and the [110] zone of fcc Ir. As expected, the new higher-charged ions were also found in these zones.

The existence of W^{5+} is now unequivocally established. It only occurs under conditions where W^{4+} is abundant; that is, at evaporation rates of the order of a monolayer per nanosecond. When several ions of the same mass pass simultaneously through the fairly large (4.75×-10^{-4} sr) probe hole their multiplicity cannot be discriminated in the output of the double-channel plate detector, so that neither oscilloscopic- nor electronic-counter readout could determine the total number of W ions evaporated. In our photographic recording of the oscilloscope traces we used the rare isotope ^{180}W (abundance 0.001 42) as a counting aid. As its time signal occurs before that of the abundant heavier W isotopes, a single ^{180}W signal stands out when, on the average, 704 W atoms have been evaporated, even when the detector is subsequently flooded by as many as a hundred heavier isotopes per shot. This method enabled us to search fairly quickly for highly charged rare tungsten ions (as well as for ions of low-concentration impurity atoms) among a quarter of a million tungsten atoms evaporated through the probe hole.

Aiming at different planes along the [111] zone, we obtained 36 W^{5+} ions with 28 counter isotope signals of $^{180}W^{4+}$ and 196 of $^{180}W^{3+}$, giving an abundance ratio $W^{5+}/(W^{3+}+W^{4+})=2.3\times10^{-4}$. In these areas the ratio of W^{4+}/W^{3+} was 0.143 as seen by the counter isotope signals. Along the [100] zone, the abundance of W^{5+} decreases to $W^{5+}/(W^{3+}+W^{4+})=1.3\times10^{-4}$, although W^{4+} almost doubles with respect to W^{3+}. In areas off these high 4+ yield zones, such as on the (166) and (144) planes, there were no W^{5+} ions found among 30 000 W^{3+} and 2000 W^{4+} ions.

Among the 157 700 tungsten ions counted via 224 ^{180}W ions in the [111]-zone series, there were also two signals representing W^{6+}, with an abundance ratio of $W^{6+}/(W^{3+}+W^{4+})=1.3\times10^{-5}$. This figure is, of course, statistically uncertain. For the matter of record, there were also thirteen signals of Mo^{3+} and Mo^{2+}, indicating an 82-ppm Mo impurity of our tungsten specimen. This small number, together with a low count of C^{2+} and C^{+}, makes it very unlikely that our W^{5+} abun-

TABLE I. Isotopic distribution of the 36 observed W^{5+} ions and natural isotope distribution of W.

Isotope	Observed number of W^{5+}	Observed percent of W^{5+}	Natural abundance (%)
180	...	...	0.14
182	13	36	26.4
183	4	11	14.4
184	13	35	30.6
186	6	16	28.4

dance is falsified by MoC^{3+}, which for the three heavier Mo isotopes would give a close overlap, but still separable with our mass resolution of better than 1/1000. The reliability of our W^{5+} data is ascertained by the observed isotope distribution, as shown in Table I, which gives a statistically satisfactory representation of the natural distribution of W isotopes, in spite of the small number of only 36 particles.

The extremely high evaporation rates employed for quickly evaporating large numbers of tungsten atoms may not really be necessary for obtaining the observed W^{5+} abundance. Two W^{5+} ions or an abundance of 3×10^{-4} were obtained at much lower rates as characterized by a yield of 136 W^{2+}, 6300 W^{3+}, and 137 W^{4+}. While most of our data were taken with the tip at 85 K there seemed to be no significant increase in the W^{5+} abundance at 28 K. Some experiments were carried out in the presence of 10^{-6} Torr He as an imaging gas, but none of the fivefold or fourfold charged ions were WHe compounds, in contrast to the abundant WHe^{3+} species.[13]

A less extensive search for highly charged ions was made with tantalum. This metal does not offer a convenient low-abundance isotope as a counting aid (^{180}Ta has a too-low abundance of 1.2×10^{-4}). Among an estimated 2×10^{4} Ta^{3+} ions and 2×10^{3} Ta^{4+}, we found four signals at 36.2 amu, representing Ta^{5+}, or an abundance of roughly 2×10^{-4}. These ions were coming from the edge of (112) towards (114), but not from (102), all regions that image brightly with helium. In the presence of this gas, the well-known $TaHe^{3+}$ is abundant, but there were no $TaHe^{4+}$ among 200 Ta^{4+} ions. Our spectra also gave three signals at 31.0 amu, indicating Nb^{3+} as a 125-ppm impurity. As the Ta specimen also contained oxygen, seen by a few ions of TaO^{3+}, TaO_2^{3+}, TaO^{4+}, and TaO_2^{4+}, there is a remote possibility that NbO^{3+} would also be present. However, its mass-to-charge ratio of 36.33 amu would have allowed us to distinguish it from Ta^{5+} at 36.20 amu. In our atom probe with a 15-kV tip, these two species would have a TOF difference of 17 nsec, while we can resolve ± 2 nsec.

Hafnium, as the element preceding Ta and W in the periodic table, was of considerable interest. Our tip material contained 1% Zr, appearing as Zr^{+}, Zr^{2+}, and Zr^{3+}. When the tip had been annealed in the residual gas in the 10^{-9}-Torr range, mostly CO, it picked up impurities which diffused throughout the inspected tip volume, so that about 3% of the Hf atoms appeared as HfC^{3+}, HfC_2^{3+}, HfO^{3+}, and HfO_2^{3+}, and there were also a total of 1% of C^{2+}, C^{+}, and O^{+} ions. Hafnium evaporates mostly as Hf^{3+}, and among 3000 of these ions we found 20, $6.7\times10^{+3}$ Hf^{4+} ions. We doubt that four signals between 34.7 and 35.7 amu were due to Hf^{5+}, which would overlap with ZrC^{3+} and ZrO^{3+} isotopes. Indeed these signals were not seen with another Hf sample under better vacuum conditions as indicated by the absence of C^{2+}, C^{+}, and O^{+}. In the presence of helium as an imaging gas $HfHe^{3+}$ is abundant.

Turning to the heavier 5*d* transition metals, with rhenium we could not find any higher charges than the well-known Re^{4+}. This metal has a particularly high evaporation field in W–25%-Re or W–3%-Re alloys. About 10^{4} Re ions were field-evaporated through the probe hole, with the ^{180}W isotope used as a counting aid in the alloys, and with advantage taken of the capability of our energy-focused atom probe of completely separating the ^{185}Re and ^{187}Re isotopes from the adjacent W isotopes. With a pure Re tip in the absence of a counting aid the Re^{4+}/Re^{3+} ratio was estimated to be 0.02. A total of 500 Re^{4+} were obtained, but no Re^{5+} within a detection limit of 5×10^{-5}.

Iridium was so far known to field-evaporate as Ir^{2+} and Ir^{3+}. When we searched along the [110] zone known for a higher abundance of Ir^{3+} we also found Ir^{4+}. This metal, too, has no convenient counting isotope so that a quantitative abundance determination of the rare Ir^{4+} is difficult. However, our Ir sample also gave some signals at 51.5 and 34.33 amu corresponding to Rh^{2+} and Rh^{3+}. This impurity shows up as an extra bright atom spot in the helium field-ion image, and, under the assumption that all Rh atoms in the surface are visible, their concentration was estimated to be about 100 ppm. In a long evaporation sequence, there were twice as many rhodium ions as Ir^{4+} ions, so the relative abundance of the latter is 5×10^{-5}.

Platinum is a very good material for employing the counting-aid isotope technique, with ^{192}Pt at 7.8×10^{-3} abundance (^{190}Pt with 1.27×10^{-4} is too rare). However, even at high evaporation rates and aiming at the [110] zone where we found 21 times more Pt^{2+} than Pt^{3+}, there were no fourfold charged ions. We inspected 10^5 Pt atoms, and the sample contained 680 ppm Rh and 270 ppm Pd as impurities. It was noted that the Rh signals frequently appeared on sequential oscilloscope traces, indicating clustering of two to four Rh atoms in the matrix, while Pd did not exhibit this effect.

Gold proved to be a difficult material for our search. The absence of a counting-aid isotope and fast field evaporation in bursts made even an estimate of the number of atoms evaporated quite inaccurate. Besides the well-known, about equally abundant Au^+ and Au^{2+}, the highest charged ion was Au^{3+}, of which 600 ions were counted among an estimated 10^4 gold atoms.

We realize that the abundances given for all our newly found, highly charged ions are only order-of-magnitude numbers. For Hf, Re, and Au we may have missed crystallographic areas where more of these ions originate, although this is unlikely. Imaging the entire tip surface by field-desorption microscopy with the channel plate screen gated for one ion species fails here because of the poor mass resolution and the large number of noise or artifact spots that far exceed the very rare highly charged ions. Our findings are not important for analytical applications of the atom probe, except for demonstrating that ion species in the 10^{-5} concentration range can be safely detected; but they suggest that a new look be taken at the theory of field evaporation. At the evaporation field, the classical electrostatic charge density at the metal surface is only about one-half an electronic charge per surface atom; thus it is difficult to conceive how fourfold to sixfold charged ions can come off the surface, requiring total ionization energies $\sum I_n$ of 194 eV for W^{6+}, 133 eV for Ta^{5+}, and 79 eV for Hf^{4+}, while the energy gain $n\varphi$ by the return of the six, five, or four electrons to the metal of work function φ is less than 30 eV.

A look at the electronic configurations of the metals studied here (Table II) shows that, for the group Hf, Ta, and W, all 6*s* and 5*d* electrons are removed in the highest stage of ionization. In the second half of that period from Re to Au (we had no osmium sample), there are the 6*s* electrons and only two electrons of the 5*d* shell removed in the highest ionization state. We may speculate that in field evaporation the transition of several valence electrons from the *d* shell occurs simultaneously and so fast that their energy levels, valid for slow, sequential ionization as expressed in the ionization potentials of the various higher charge stages, are irrelevant. The adiabatic ionization process involves a pairwise electron transition out of the *d* shell as indicated by the even number of these electrons, except in the case of tantalum.

TABLE II. Number of 5*d* and 6*s* electrons in the outer shells and highest ionic charge n^+ in field evaporation.

Metal	5*d*	6*s*	n^+	Max. abundance of highest n
Hf	2	2	4	6.7×10^{-3}
Ta	3	2	5	2×10^{-4}
W	4	2	6	1.3×10^{-5}
Re	5	2	4	2×10^{-2}
Os	6	2	-	•••
Ir	7	2	4	5×10^{-5}
Pt	9	1	3	5×10^{-2}
Au	10	1	3	6×10^{-2}

The authors wish to express their appreciation to Mr. S. Brooks McLane for his assistance in taking the data.

*This work has been supported by the National Science Foundation, Grant No. DMR 72-02925 A03.

[1]E. W. Müller, Naturwissenschaften 29, 533 (1941).
[2]E. W. Müller, Phys. Rev. 102, 618 (1956).
[3]D. G. Brandon, Surface Sci. 3, 1 (1965).
[4]M. Vesely and G. Ehrlich, Surface Sci. 34, 547 (1973).
[5]R. Gomer, J. Chem. Phys. 31, 341 (1959).
[6]D. McKinstry, Surface Sci. 29, 37 (1972).
[7]E. W. Müller, J. A. Panitz, and S. B. McLane, Rev. Sci. Instrum. 39, 83 (1968).
[8]E. W. Müller, in *Field Ion Microscopy in Physical Metallurgy and Corrosion*, edited by R. F. Hochman, E. W. Müller, and B. Ralph (Georgia Institute of Technology, Atlanta, 1968), p. 59.
[9]E. W. Müller, S. B. McLane, and J. A. Panitz, in *Proceedings of the Fourth European Regional Conference on Electron Microscopy, Rome, Italy*, edited by O. S. Bocciarelli (Tipographia Poliglotta Vaticana, Rome, 1968), Vol. 1, p. 135.
[10]S. S. Brenner and J. T. McKinney, Appl. Phys. Lett. 13, 29 (1968).
[11]E. W. Müller and S. V. Krishnaswamy, Rev. Sci.

Instrum. 45, 1053 (1974); E. W. Müller, in *Methods of Surface Analysis*, edited by A. W. Czanderna (Elsevier, Amsterdam, 1975), Chap. 8, pp. 328–385.

[12]J. A. Panitz, J. Vac. Sci. Technol. 12, 210 (1975).

[13]S. V. Krishnaswamy, S. B. McLane, and E. W. Müller, J. Vac. Sci. Technol. 13, 665 (1976).

Paramagnetic Susceptibility of Disordered N-Methyl-Phenazinium Tetracyanoquinodimethanide*

George Theodorou and Morrel H. Cohen

Department of Physics and The James Franck Institute, The University of Chicago, Chicago, Illinois 60637

(Received 26 February 1976)

The organic charge-transfer salt N-methyl-phenazinium tetracyanoquinodimethanide is described in terms of a one-dimensional disordered Hubbard model. For low temperatures and small transfer integrals this model reduces to a disordered Heisenberg antiferromagnet. The magnetic susceptibility of the latter can be described adequately by the disordered classical Heisenberg model. Fitting of susceptibility data by the one-dimensional classical Heisenberg model provides us with values of $t = 0.055$ eV, $U_{\text{eff}} = 0.130$ eV, and $\sigma = 0.136$ eV for the parameters of the original Hubbard Hamiltonian.

The paramagnetic susceptibilities, χ_p, of the high-conductivity charge-transfer salts[1-5] N-methyl-phenazinium tetracyanoquinodimethanide (NMP-TCNQ), quinolinium tetracyanoquinodimethanide [Qn(TCNQ)$_2$], and acridinium tetracyanoquinodimethanide [Ad(TCNQ)$_2$] depend weakly on temperature at high temperatures, but behave[1] as $\chi_p \propto 1/T^\gamma$ with $\gamma < 1$ at low temperatures. Figure 1 shows various experimental results for NMP-TCNQ, whose magnetic properties are the subject of this Letter. The crystal structure[6,7] of NMP-TCNQ consists of chains of closely stacked $TCNQ^-$ anions separated by chains of NMP^+ cations. The small intrachain $TCNQ^-$ spacing and large interchain distances lead to pseudo one-dimensional motion of electrons along the individual stacks. Bloch, Weisman, and Varma[8] first recognized that structural disorder is important for the conductivity of NMP-TCNQ. X-ray studies showed that the orientation of the asymmetric NMP^+ cations can be either random,[6,7] with a variable degree of disorder, or ordered.[9] We attribute the large variability in susceptibility throughout the whole temperature region, Fig. 1, to the intrinsic structural disorder.

Epstein *et al.*[3] have argued that at low temperatures their data can be quantitatively described by the half-filled periodic Hubbard model. Their explanation, however, cannot account for the rapid growth of the susceptibility observed by others. Butler, Wudl, and Soos[10] found their NMR data to be consistent with the assumption of partial charge transfer, and attributed the low-temperature growth of χ_p to electrons localized on 5% of the NMP sites. This picture cannot explain the variability in the susceptibility and does not give the $1/T^\gamma$ behavior. Bulaevskii *et al.*[1] proposed a phenomenological model which they based on the disordered Heisenberg model with a nonsingular probability distribution $P(J)$ of the coupling constant J. A canonical transformation reduces this model to one of interacting spinless fermions. They assumed that the Fermi-liquid theory holds for the interacting spinless fermions and that the

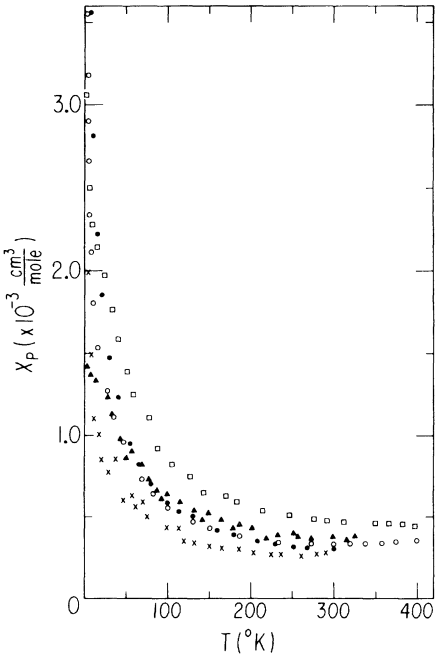

FIG. 1. Paramagnetic susceptibility data of NMP-TCNQ as a function of temperature. □, from Ref. 4; ●, from Ref. 2; ○, from Ref. 1; ▲, from Ref. 3; and x, from Ref. 5.